Histopathobiome – integrating histopathology and microbiome data via multimodal deep learning

Agata Polejowska AGATA.POLEJOWSKA@RADBOUDUMC.NL
Annemarie Boleij ANNEMARIE.BOLEIJ@RADBOUDUMC.NL
Francesco Ciompi FRANCESCO.CIOMPI@RADBOUDUMC.NL

Department of Pathology, Radboud University Medical Center, Nijmegen, The Netherlands

Abstract

We introduce *Histopathobiome*, a term representing the integration of histopathology and microbiome data to explore tissue-microbe interactions. Using a dataset of colon biopsy whole-slide images paired with microbiota composition samples, we assess the benefits of combining these modalities. Initially, we evaluate the unimodal performance of state-of-the-art algorithms using vectors representing bacterial species abundances or histopathology slide-level embeddings. We compare single-modality models with bimodal networks that use various fusion strategies. Our results prove that histopathology and microbiome data are complementary. By yielding improved performance over single-modality approaches, bimodal deep learning models can learn cross-modal interpretable tissue-microbe patterns.

Keywords: Computational pathology, microbiome, multimodality, fusion, deep learning, Inflammatory Bowel Disease, Ulcerative Colitis

1 Introduction

We investigate tissue-microbe interactions in Inflammatory Bowel Disease (IBD) through the application of multimodal learning techniques fusing histopathology and microbiota abundance representations. The rationale for combining these two modalities lies in their complementary nature. Histopathology provides detailed insights into tissue morphology and pathological changes, such as ulcers, inflammation, and crypt distortion, which are important in diagnosing and staging diseases like Ulcerative Colitis (UC) and Crohn's Disease (CD), the IBD subtypes. However, some features might overlap between them making it more challenging to use only histopathology for definite diagnostics (Kellermann and Riis (2021)). Also, histopathology may not capture the underlying microbial composition and dynamics that can influence these pathological changes. Conversely, microbiome data can reflect the community of microorganisms residing in the tissue and provide information on microbial composition and potential dysbiosis — an imbalance in microbial populations often associated with diseases (Nishida et al. (2018); Wei et al. (2021)). For example, known microbes, such as Escherichia coli and Bacteroides fragilis, have been implicated in UC pathogenesis (Bruggeling et al. (2023)). Yet, relying solely on microbiome data for diagnosis is challenging due to the dynamic nature of microbial communities, which can be influenced by various factors and subjected to the quality of preparation methods (Garrett (2019); Hajjo et al. (2022); Schlaberg (2019)).

Thanks to recent advancements in computational pathology and metagenomics sequencing technology, the horizons for artificial intelligence to unravel the complexities behind

diseases have been broadened. Computational pathology models are now capable of generating efficient slide-level representations in the form of embeddings, enabling compression of large histology slides into one vector (Xu et al. (2024); Song et al. (2024)). Meanwhile, metagenomics sequencing can offer microbial profiles (Shi et al. (2022)). However, integrating heterogeneous data, such as histopathology and microbiome data, into a common, learnable representation is still a challenge. Over the years, several fusion techniques and multimodal architectures have been proposed. The basic categories of fusion include early fusion that combines raw data early in the pipeline using simple operations like concatenation, but this may remove structural modality-specifc information. Another popular method is the late fusion that uses outputs from separate models trained on different modalities, preserving modality-specific features but potentially missing cross-modal interactions. Recent multimodal frameworks (Hemker et al. (2023), Jaume et al. (2024)) address common drawbacks encountered in basic fusion architectures and demonstrate the potential to efficiently capture cross-modal information while preserving modality-specific features and being able to outperform other baselines.

To our knowledge, our work presents the first application of deep learning to integrate histopathology and microbiome data. The primary aim is to verify whether a deep learning model can depict their complementary nature and thus improve classification of UC versus non-IBD patients. We leverage advancements in computational pathology and metagenomics to use a common representation format. We conduct experiments on each modality independently using well-established models. We design and adapt distinct bimodal models by testing different fusion techniques while exploring the model's ability to capture cross-modal patterns. The results are concluded not only based on various performance metrics but also by including interpretability measures as the focus is also placed on discovering new tissue-microbe interactions to broaden the understanding of IBD.

2 Methods

Dataset The dataset originates from an investigation of bacterial oncotraits and UC (Bruggeling et al. (2023)). Biopsies were collected from the ascending and descending colon of 80 UC patients and 35 non-IBD controls. The detailed bacterial species composition from clinical tissue samples was derived thanks to isolating the bacterial DNA using an optimized method and shotgun metagenomic sequencing (Bruggeling et al. (2021)). Haematoxylin and Eosin (H&E) stained pathology slides were analyzed together with other techniques. For our experiments, from the original study we selected two modalities: histopathology (H&E) images and relative abundances of bacteria species at a genus level. Initially, 234 tissue samples were collected, from which we excluded 32 samples due to being out of focus. For image processing, tissue samples were divided into non-overlapping patches of 224×224 pixels at a spacing of 0.5 micrometers per pixel (MPP), resulting in a total of 30644 patches for the entire dataset, with a median of 150 patches per sample. Using the extracted patches and their coordinates, we leveraged a foundation model's ability to generate slide-level representations. Specifically, we used a recent Prov-GigaPath model pretrained on a large pathology dataset in which bowel tissue is the second most common tissue type (Xu et al. (2024)). For the second modality, we use raw bacteria species composition values stored in tabular form. Figure 1 provides a high-level overview of the data. We use pairs of microbiota

composition from the tissue sample and the corresponding tissue histopathology image from the left and right side of the colon. For each histopathology whole-slide image, we used 768 values in the feature vector to serve as a slide-level representation. For microbiome data, we obtained a vector length of 432 representing relative abundance values for each of 432 bacteria species at a genus level.

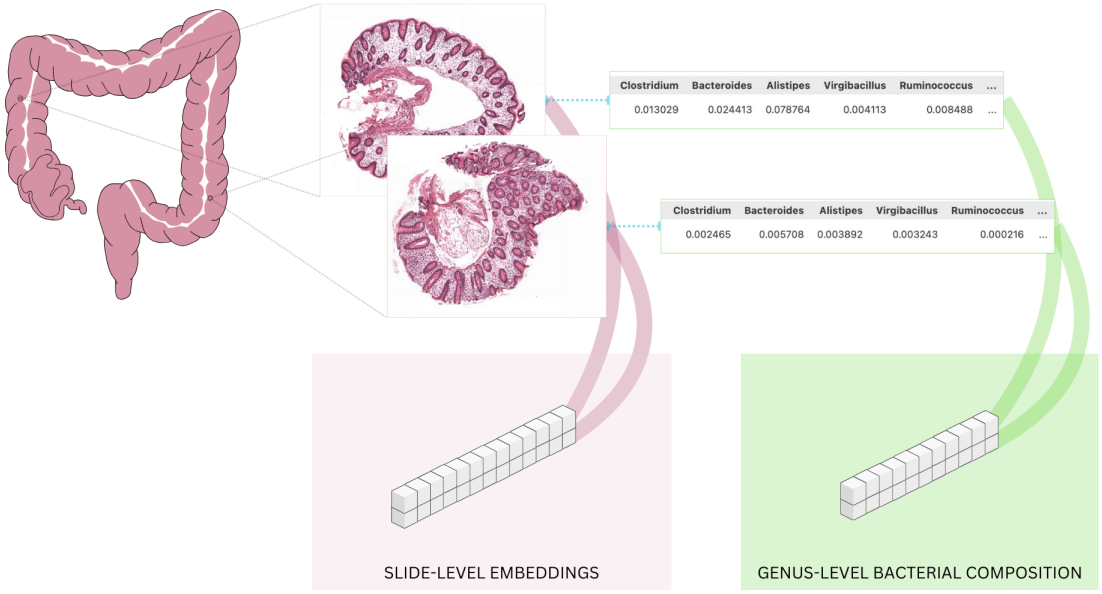

Figure 1: High-level visualization of the dataset preparation from colon biopsies images and microbiota composition to vector representations.

Unimodal models For both, slide-level embeddings and genus-level bacterial composition, we employ deep learning models such as Feature Tokenizer + Transformer (FT-Transformer) (Gorishniy et al. (2021)), Self-attentive Neural Networks (AutoInt) (Song et al. (2019)) and Gated Adaptive Network for Deep Automated Learning of Features (GANDALF) (Joseph and Raj (2022)) within PyTorch Tabular framework (Joseph, 2021). For comparison, we also check the performance of an *ensemble* gradient-based machine learning approach, namely GRANDE (Marton et al. (2023)). From the deep learning approaches, FT-Transformer was chosen for the experiments as it has proven to be a versatile model for a wide range of tabular data problems despite being defined as a simple adaptation of the Transformer architecture to the tabular data domain (Gorishniy et al. (2021)). The AutoInt model is also included in the experiments due to its ability to learn feature interactions in an explicit manner via using an interacting layer which determines the features' relevance. GANDALF was selected due to its reported robust feature selection and learning capabilities, excelling in datasets with numerous features or complex feature-target relationships. Also, empirical results demonstrate GANDALF's better performance over a plain Multi-layer Perceptron (MLP) (Joseph and Raj (2022)).

Bimodal models For our use case, we define multimodal, specifically bimodal, models as networks capable of learning crossmodal information from two inputs coming from two different data domains. Despite having transformed the image data into a common format aligned with the microbiota modality, the meaning of the values is different and each modality requires distinct registration and derivation techniques. Firstly, we use the GANDALF architecture on combined histopathology embeddings and microbiota abundances together as parallel input fed into the network. This network was selected as it performed the best among the introduced tabular models showing that it can learn from a data structure with 1200 features. Next, we design and test vanilla fusion models. The early fusion model firstly combines histopathology features and microbiota features via a concatenation operation. The combined input undergoes layer normalization to stabilize the training process. Then, linear layers are used to project the values to a hidden representation. This approach allows the model to leverage complementary information from both inputs right from the initial layers. The late fusion model is built with separate networks to process each input feature independently. The outputs of these two networks are concatenated and fed into a simple fully connected fusion network. This late fusion approach can allow the model to process information from histopathology and microbiome data independently before integrating them at a later stage. Also, we employ more complex fusion techniques. We adapt the Hybrid Early-fusion Attention Learning Network (HEALNet) (Hemker et al. (2023)) for learning from whole-slide image embeddings and microbiota abundance vectors, both defined in a tabular structure for the network input. For this model, we use default parameters configuration, with Fourier data encoding. The next network tested, inspired by SurvPath work (Jaume et al. (2024)), is comprised of a self-normalizing neural network (SNN) block for encoding microbiota vectors and a simple linear projection layer for WSI embeddings. The tokens from those blocks are concatenated and fed into the Nystrom Attention (NA) module. The embeddings obtained after this self-attention approximation are used in the network learning process.

Training The models are trained to classify whether a sample belongs to individuals with UC or a non-IBD control group. As this is a binary classification, each model network uses Binary Cross Entropy loss during the learning procedure. The length of the training is dependent on the convergence speed and criteria. For this, an early stopping callback is set to stop the learning when the validation loss function does not decrease further after 5 consecutive epochs (patience number equal to 5). The maximum number of epochs is set to 50 with a batch size of 16, a learning rate equal to 0.001 and an Adam optimizer.

Validation and testing KFold (k=5) cross-validation is performed. During the validation and testing phase, group ratios are maintained in each split without patient overlap. The metrics include: the Area Under the Receiver Operating Characteristic Curve (AUC), Average Precision (AP) to summarize a precision-recall curve, and the Matthews Correlation Coefficient (MCC). We include the MCC score, in a normalized form, as it has been reported to address the other metrics drawbacks (Chicco and Jurman (2023, 2020)). However, as there is also evidence that the MCC alone might not be a suitable measure for an imbalanced dataset (Zhu (2020)), we also compute AP and AUC. The metrics values reported for cross-validation are the mean and standard deviation measured across all folds.

For a fixed test set, the best performing model based on the cross-validation mean MCC score is selected, and metrics on the test set for this model are reported.

Interpretability To gain insights into tissue-microbe relations, we design a pipeline to interpret the model's decisions. Based on the conducted experiments, and to be able to look into the unimodal model feature importance assignment process as well as the model decisions that use both modalities, we select the GANDALF model. We use interpretability methods, such as Feature Ablation and GradientShap, implemented in Captum framework (Kokhlikyan et al. (2020)) available for the models via PyTorch Tabular interface (Joseph (2021)). When whole-slide image embedding indices are used as features, we perform patch ablation, checking which patch contributes to the greatest change in the corresponding value in the feature vector. The explanations are run on the whole test set.

3 Results and Discussion

Based on Table 1 the most relevant difference in metrics values is observed for the test dataset where the GANDALF model provides the leading results. Figure 2 indicates that Absiella, Leuconostoc, Lactococcus and Sporanaerobacter have the highest attibutions for the UC vs. non-IBD patients group classification using GANDALF's predictions.

Table 1: Metrics calculated for microbiota abundances input modality.

		Cross-validation			Test		
Model	Params	AUC	AP	MCC	AUC	AP	MCC
AutoInt	56.1 K	$\mathbf{0.5262 \pm 0.0901}$	$\mathbf{0.7721 \pm 0.0867}$	0.5000 ± 0.0528	0.5031	0.7884	0.5303
FT-Transformer	300 K	0.5110 ± 0.0274	0.7563 ± 0.1040	$\mathbf{0.5175 \pm 0.0298}$	0.5078	0.7929	0.5065
GANDALF	6.7 M	0.5183 ± 0.1017	0.7603 ± 0.1016	0.5096 ± 0.0470	**0.6161**	**0.8317**	**0.5494**
GRANDE	NA	0.4969 ± 0.0054	0.7499 ± 0.1049	0.4956 ± 0.0076	0.5	0.7903	0.5

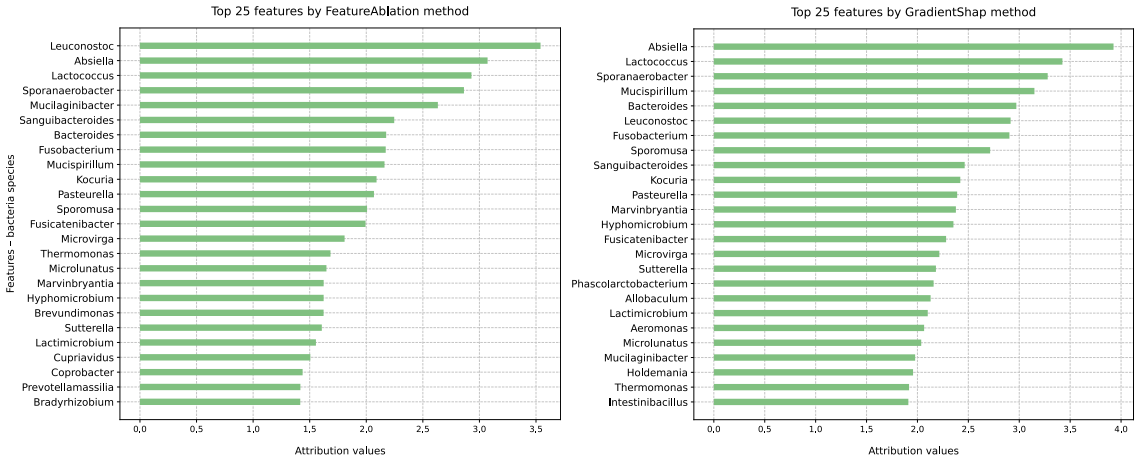

Figure 2: Attribution values for each feature based on two interpretability methods.

Results in Table 2 show that the self-attentive neural network (AutoInt) outperforms other models in this classification task based on whole-slide image embeddings. For con-

gruity, embedding index relevance is computed for the GANDALF model (Figure 3), so that the most important patches for a given embedding index can be verified. We provide visualizations of the most impactful patches (Figure 5) for index 399 value since it appears as the feature with one of the highest attribution values in both settings.

Table 2: Metrics calculated for histopathology slide-level embeddings input modality.

		Cross-validation			Test		
Model	Params	AUC	AP	MCC	AUC	AP	MCC
AutoInt	89.0 K	0.5537 ± 0.0521	$\mathbf{0.7363 \pm 0.0995}$	$\mathbf{0.5588 \pm 0.0582}$	**0.6259**	**0.7837**	**0.6358**
FT-Transformer	323 K	$\mathbf{0.5548 \pm 0.0546}$	0.7358 ± 0.1060	0.5725 ± 0.0728	0.5814	0.7634	0.6326
GANDALF	21.3 M	0.5247 ± 0.0940	0.7308 ± 0.1009	0.5445 ± 0.0830	0.5444	0.7477	0.5577
GRANDE	NA	0.4921 ± 0.0559	0.7112 ± 0.1105	0.4971 ± 0.0954	0.5315	0.7424	0.5618

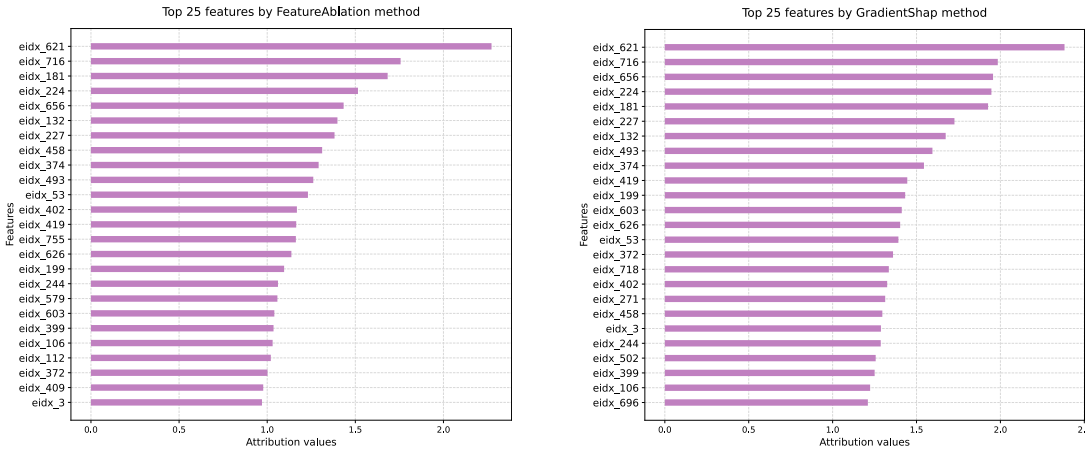

Figure 3: Attribution values for each feature computed using two interpretability methods.

According to the obtained results, microbiome-only data encodes more informative values for classifying IBD patients than histopathology slides embeddings only. However, the metrics values reflect that it is still a challenge to use a single modality for an optimal performance, which may indicate that performance gains can be achieved by using fusion techniques to merge both modalities and to capture interconnected patterns.

Table 3: Metrics calculated for different multimodal algorithms.

		Cross-validation			Test		
Model	Params	AUC	AP	MCC	AUC	AP	MCC
GANDALF*	51.9 M	0.6412 ± 0.1438	0.7962 ± 0.1045	0.5519 ± 0.0604	0.6733	0.8133	0.5777
Early Fusion	617 K	0.6942 ± 0.0997	0.8488 ± 0.0999	0.5606 ± 0.0471	0.6578	0.8572	0.6451
Late Fusion	1.1 M	0.7345 ± 0.0431	$\mathbf{0.8785 \pm 0.0552}$	0.6327 ± 0.1148	0.68	**0.8689**	0.5915
NA + SNN	1.8 M	$\mathbf{0.7627 \pm 0.0790}$	0.7513 ± 0.0828	$\mathbf{0.7472 \pm 0.0844}$	**0.8015**	0.8357	**0.7353**
HEALNet	32.2 M	0.7472 ± 0.0844	0.6949 ± 0.0925	$\mathbf{0.7472 \pm 0.0844}$	0.7353	0.7151	**0.7353**

For multimodal performance (Table 3), the self-normalizing network together with self-attention approximation module gives the best results on the test dataset given AUC and MCC metrics. Simpler approaches, like Early Fusion and Late Fusion, show even better performance, according to AP values, compared to more complex ones. Also, the GANDALF model benefits from learning on merged representations achieving improved results on the test set based on AUC and MCC values in contrast to when used for single-modality experiments.

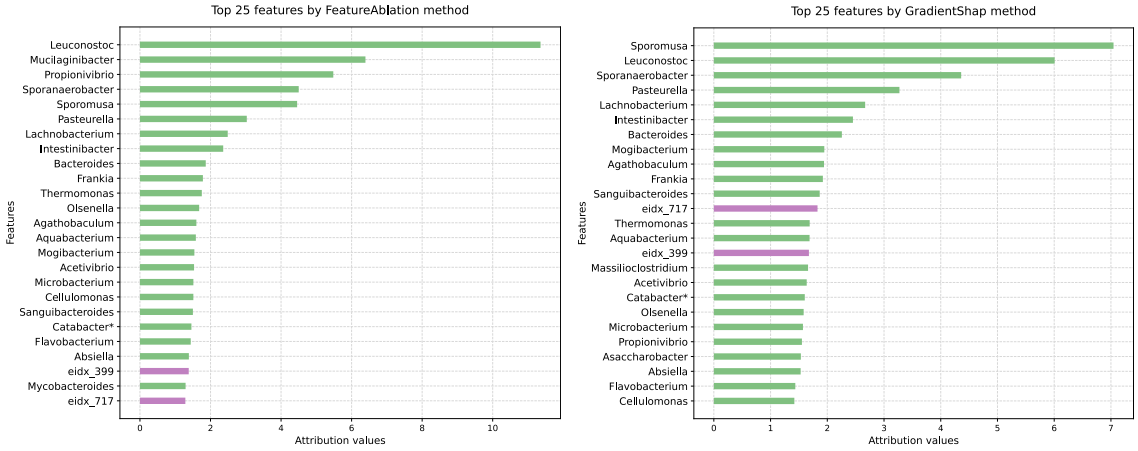

Figure 4: Attribution values for each feature based on two interpretability methods.

In Figure 4, it can be seen that microbiota abundances largely dominate the model's decision making process. Index 399 and 717 of whole-slide image embeddings appear twice in both interpretability methods. Values in those indicies are mostly impacted by the patches shown in Figure 5. It can be observed that more focus is placed on colon crypts in the case of non-IBD tissue samples.

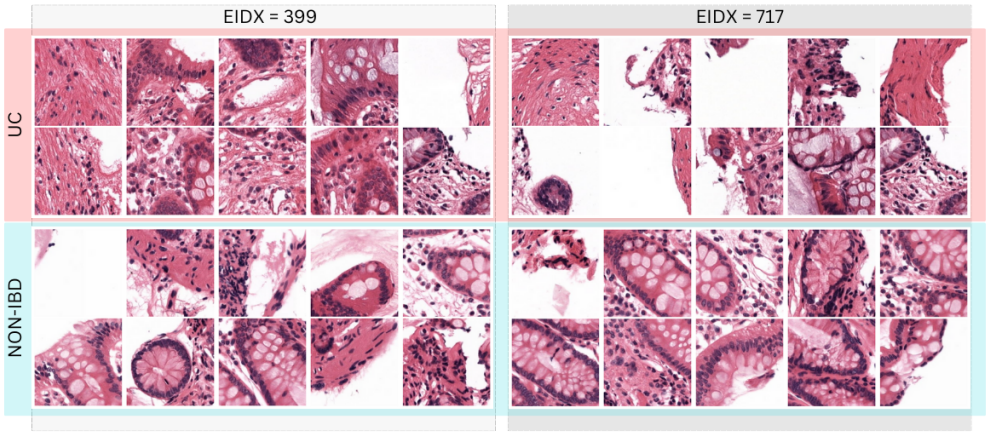

Figure 5: Most influential patches from UC and non-IBD patient on embeddings' values based on embedding's indicies with the highest attribution value.

When compared to input based solely on microbiota (see Figure 2), Leuconostoc bacteria continue to be ranked at the top. Interestingly, a recent study has reported that Leuconostoc species, which are found in kimchi (Moon et al. (2023)), are capable of attenuating the inflammatory responses associated with colitis. Mucilaginibacter has the second highest attribution value when conducting features ablation. The current research does not indicate that this type of bacteria plays a significant role in UC, however it is capable of fermenting glucose and sucrose (Pankratov et al. (2007)), which are the types of simple carbohydrates which when often included in a diet, can be highly associated with IBD (Shon et al. (2023))). Furthermore, when adding a second type of data, some bacteria like Lachnobacterium and Aquabacterium become more important, while others like Marvinbryantia and Kocuria no longer appear in the top rankings. This shows that a multimodal approach can reveal different insights into how bacteria interact with the tissue.

4 Limitations

Further enhancement of model performance can be achieved through the implementation of alternative architectures and tuning of hyperparameters, potentially leading to performance gains. As model performance improves, the reliability of interpretability method outputs is expected to increase. However, the selection of interpretability methods requires careful consideration. For instance, our tests with KernelShap demonstrated a higher impact and prevalence of the histopathology modality in the attribution plots. Additionally, the exploration of other pretrained models for generating whole-slide image embeddings warrants further investigation.

5 Conclusions

In conclusion, this study contributes the foundation for future optimizations of multimodal architectures, with explainability and interpretability measures, in the new *Histopathobiome* learning and exploration application. The experimental results suggest that the metrics values obtained might reflect the inherent complexity of the dataset or IBD in general. Nevertheless, combining different features by employing multimodal deep learning can lead to better results compared to single-modality-based classification, thus proving *Histopathobiome* potential. Furthermore, we demonstrated the exploration of tissue-microbe patterns, using interpretability techniques, which can be compared to existing literature. This application of artificial intelligence shows promise in uncovering previously unknown associations. Moreover, with appropriate datasets, this approach may extend to other gut-related diseases and conditions affecting brain health via the gut-brain axis, offering even greater potential for impactful discoveries. Understanding the biological environment and the coexistence with bacteria could also lead to exploring their therapeutic potential to treat various diseases as we deepen our understanding of their impact with the help of deep learning.

Acknowledgments and Disclosure of Funding

This work was supported by the HEREDITARY Project, as part of the European Union's Horizon Europe research and innovation programme under grant agreement No GA 101137074.

References

Carlijn E Bruggeling, Daniel R Garza, Soumia Achouiti, Wouter Mes, Bas E Dutilh, and Annemarie Boleij. Optimized bacterial dna isolation method for microbiome analysis of human tissues. *Microbiologyopen*, 10(3):e1191, 2021.

Carlijn E Bruggeling, Maarten Te Groen, Daniel R Garza, Famke van Heeckeren Tot Overlaer, Joyce PM Krekels, Basma-Chick Sulaiman, Davy Karel, Athreyu Rulof, Anne R Schaaphok, Daniel LAH Hornikx, et al. Bacterial oncotraits rather than spatial organization are associated with dysplasia in ulcerative colitis. *Journal of Crohn's and Colitis*, 17(11):1870–1881, 2023.

Davide Chicco and Giuseppe Jurman. The advantages of the matthews correlation coefficient (mcc) over f1 score and accuracy in binary classification evaluation. *BMC genomics*, 21:1–13, 2020.

Davide Chicco and Giuseppe Jurman. The matthews correlation coefficient (mcc) should replace the roc auc as the standard metric for assessing binary classification. *BioData Mining*, 16(1):4, 2023.

W. Garrett. The gut microbiota and colon cancer. *Science*, 364:1133 – 1135, 2019. doi: 10.1126/science.aaw2367.

Yury Gorishniy, Ivan Rubachev, Valentin Khrulkov, and Artem Babenko. Revisiting deep learning models for tabular data. *Advances in Neural Information Processing Systems*, 34:18932–18943, 2021.

R. Hajjo, D. Sabbah, and A. A. Al Bawab. Unlocking the potential of the human microbiome for identifying disease diagnostic biomarkers. *Diagnostics*, 12, 2022. doi: 10.3390/diagnostics12071742.

Konstantin Hemker, Nikola Smidjievski, and Mateja Jamnik. Healnet–hybrid multi-modal fusion for heterogeneous biomedical data. *arXiv preprint arXiv:2311.09115*, 2023.

Guillaume Jaume, Anurag Vaidya, Richard J Chen, Drew FK Williamson, Paul Pu Liang, and Faisal Mahmood. Modeling dense multimodal interactions between biological pathways and histology for survival prediction. In *Proceedings of the IEEE/CVF Conference on Computer Vision and Pattern Recognition*, pages 11579–11590, 2024.

Manu Joseph. Pytorch tabular: A framework for deep learning with tabular data, 2021.

Manu Joseph and Harsh Raj. Gandalf: Gated adaptive network for deep automated learning of features. *arXiv preprint arXiv:2207.08548*, 2022.

Lauge Kellermann and Lene Buhl Riis. A close view on histopathological changes in inflammatory bowel disease, a narrative review. *Digestive Medicine Research*, 4, 2021.

Narine Kokhlikyan, Vivek Miglani, Miguel Martin, Edward Wang, Bilal Alsallakh, Jonathan Reynolds, Alexander Melnikov, Natalia Kliushkina, Carlos Araya, Siqi Yan, et al. Captum: A unified and generic model interpretability library for pytorch. *arXiv preprint arXiv:2009.07896*, 2020.

Sascha Marton, Stefan Lüdtke, Christian Bartelt, and Heiner Stuckenschmidt. Grande: Gradient-based decision tree ensembles. *arXiv preprint arXiv:2309.17130*, 2023.

Hye-Jung Moon, Suk-Heung Oh, Ki-Bum Park, and Youn-Soo Cha. Kimchi and leuconostoc mesenteroides drc 1506 alleviate dextran sulfate sodium (dss)-induced colitis via attenuating inflammatory responses. *Foods*, 12(3):584, 2023.

Atsushi Nishida, Ryo Inoue, Osamu Inatomi, Shigeki Bamba, Yuji Naito, and Akira Andoh. Gut microbiota in the pathogenesis of inflammatory bowel disease. *Clinical journal of gastroenterology*, 11:1–10, 2018.

Timofei A Pankratov, Brian J Tindall, Werner Liesack, and Svetlana N Dedysh. Mucilaginibacter paludis gen. nov., sp. nov. and mucilaginibacter gracilis sp. nov., pectin-, xylan-and laminarin-degrading members of the family sphingobacteriaceae from acidic sphagnum peat bog. *International Journal of Systematic and Evolutionary Microbiology*, 57(10):2349–2354, 2007.

R. Schlaberg. Microbiome diagnostics. *Clinical chemistry*, 2019. doi: 10.1373/clinchem.2019.303248.

Yu Shi, Guoping Wang, H. C. Lau, and Jun Yu. Metagenomic sequencing for microbial dna in human samples: Emerging technological advances. *International Journal of Molecular Sciences*, 23, 2022. doi: 10.3390/ijms23042181.

Woo-Jeong Shon, Min Ho Jung, Younghoon Kim, Gyeong Hoon Kang, Eun Young Choi, and Dong-Mi Shin. Sugar-sweetened beverages exacerbate high-fat diet-induced inflammatory bowel disease by altering the gut microbiome. *The Journal of Nutritional Biochemistry*, 113:109254, 2023.

Andrew H Song, Richard J Chen, Tong Ding, Drew FK Williamson, Guillaume Jaume, and Faisal Mahmood. Morphological prototyping for unsupervised slide representation learning in computational pathology. In *Proceedings of the IEEE/CVF Conference on Computer Vision and Pattern Recognition*, pages 11566–11578, 2024.

Weiping Song, Chence Shi, Zhiping Xiao, Zhijian Duan, Yewen Xu, Ming Zhang, and Jian Tang. Autoint: Automatic feature interaction learning via self-attentive neural networks. In *Proceedings of the 28th ACM international conference on information and knowledge management*, pages 1161–1170, 2019.

Lai Wei, Rajan Singh, Seungil Ro, and Uday C Ghoshal. Gut microbiota dysbiosis in functional gastrointestinal disorders: Underpinning the symptoms and pathophysiology. *JGH open*, 5(9):976–987, 2021.

Hanwen Xu, Naoto Usuyama, Jaspreet Bagga, Sheng Zhang, Rajesh Rao, Tristan Naumann, Cliff Wong, Zelalem Gero, Javier González, Yu Gu, et al. A whole-slide foundation model for digital pathology from real-world data. *Nature*, pages 1–8, 2024.

Qiuming Zhu. On the performance of matthews correlation coefficient (mcc) for imbalanced dataset. *Pattern Recognition Letters*, 136:71–80, 2020.